Supporting information

In-situ Formation of ZnS/In Interphase for Reversible Zn metal anode at Ultrahigh Currents and Capacities

Chengwu Yang[a], Pattaraporn Woottapanit[a], Jin Cao[b], Yilei Yue[c], Dongdong Zhang[d], Jin Yi[e], Zhiyuan Zeng[f], Xinyu Zhang[c]*, Jiaqian Qin[a]*, Yonggang Wang[g]*

[a] Center of Excellence on Advanced Materials for Energy Storage, Metallurgy and Materials Science Research Institute, Chulalongkorn University, Bangkok 10330, Thailand

[b] College of Materials and Chemical Engineering, China Three Gorges University, Yichang, Hubei 443002, China

[c] State Key Laboratory of Metastable Materials Science and Technology, Yanshan University, Qinhuangdao 066004, P. R. China

[d] School of Materials Science and Engineering, Shenyang University of Technology, Shenyang 110870, China

[e] Institute for Sustainable Energy/College of Sciences, Shanghai University, 99 Shangda Road, Shanghai 200444, China.

[f] Department of Materials Science and Engineering, City University of Hong Kong, 83 Tat Chee Avenue, Kowloon, Hong Kong 999077, China

[g]Department of Chemistry and Shanghai Key Laboratory of Molecular Catalysis and Innovative Materials, Institute of New Energy, iChEM (Collaborative Innovation Center of Chemistry for Energy Materials), Fudan University, Shanghai 200433, China

*Corresponding Author.

E-mail: xyzhang@ysu.edu.cn (X. Zhang), jiaqian.q@chula.ac.th (J. Qin),

ygwang@fudan.edu.cn (Y. Wang)

Experimental section

Material synthesis

Preparation of ZIS. $ZnIn_2S_4$ nanosphere was prepared via a simple hydrothermal reaction process. First, 0.8 mmol of $ZnCl_2$, 1.6 mmol of $InCl_2 \cdot 4H_2O$ and 6.4 mmol of thiourea were dissolved in 60 ml aqueous solution (50 vol% ethanol) under stirring condition. Then, the above solution was transferred to 100 ml Teflon-lined stainless-steel autoclave and heated at 180 ℃ for 12 h. The resultant yellow precipitation was gathered by centrifugation after hydrothermal reaction and washed several times with deionized water and ethanol. Finally, the ZIS powder was dried at 70 ℃ for further use.

Preparation of ZISG-CC. $ZnIn_2S_4$, graphene oxide coated carbon fiber cloth was prepared via a blade-casting method. The coating slurry was fabricated by mixing $ZnIn_2S_4$, GO and polyvinylidene fluoride (PVDF) in N-methyl-2-pyrrolidone (NMP). Briefly, a certain amount of $ZnIn_2S_4$, GO and PVDF (mass ratio of 7:2:1) was added into 3 ml NMP and stirred for 2 h. Then, 1 ml of the slurry was uniformly dropped onto the surface of CC (4.5 cm × 4.5 cm) and coated using blade. The ZIS, GO-coated CC was dried at 60 ℃ for 12 h.

Preparation of Zn/ZISG-CC anode. The Zn/ZIS-GO/CC anode was prepared via an electroplating method. The electroplating process was performed on DC power

supply. A ZISG-CC sample was used as working electrode, while Zn foil was the counter electrode. The used electrolyte was 75 ml of mixture solution of $ZnSO_4$ and $NaSO_4$. The current density of electroplating was set to 1 $mA \cdot cm^{-2}$. The different capacities of Zn deposited on CC (10 $mAh \cdot cm^{-2}$ and 20 $mAh \cdot cm^{-2}$) can be achieved by altering the electroplating time. Afterwards, the Zn/ZIS-GO/CC was washed several times with deionized water and dried at 60 ℃ for 12 h.

Preparation of MnO_2-graphite cathode material. MnO_2-graphite hybrids was prepared basing the previous report of our group [1]. 4.5 g of MnO_2 powder and 0.5 g of graphite were mixed via ball-milling for 3 h with a rotation speed of 200 rpm. The mass ratio of MnO_2-graphite mixture to ceramic ball was 1:10. After that, the MnO_2-graphite hybrids were collected and severed as cathode material for AZIBs.

Material characterization

X-ray powder diffraction (XRD) was conducted on Bruker D8 advance X-ray diffractometer with Cu K radiation. Sample morphologies were observed by scanning electron microscopy (SEM. Hitachi S4800). Element composition and chemical information were analyzed by X-ray photoelectron spectroscopy (Thermo ESCALAB spectrometer). Specific surface area was measured by ASAP 2020 HD88 and water contact test was conducted on DM-CEI.

The in-situ XRD was carried out by Bruker D8 advance X-ray diffractometer using home-made electrochemical cell. The electrolyte was 2M $ZnSO_4$ and the applied current density was 5 $mA \cdot cm^{-2}$.

Theoretical calculations

All spin-polarized DFT (density functional theory) calculations were performed via Vienna ab initio simulation package (VASP). The GGA-PBE exchange-correlation functional were used to describe the electron interactions and the van der Waals (vdW) interactions were evaluated by Grimme's semiempirical DFT-D3 scheme. The cutoff energy of 500 eV was set for plane-wave basis sets. The Brillouin zones were sampled by 5×5×1 k-point grids for all models optimization. All structural relaxations were converged at 0.02 eV/ $Å^{-1}$.

Electrochemical measurements

The bare and coated CC and pure Zn foil were first cut into disc-shaped electrodes (Φ = 14 mm). Zn electrode, glass fiber separator and 2 M $ZnSO_4$ electrolyte were assembled to Zn|$ZnSO_4$ |Zn cells. To explore the morphology evolution of Zn on bare CC and ZIS-GO/CC, Zn|CC and Zn|ZISG-CC were constructed and tested at 1 mA·cm^{-2} with 10 mAh·cm^{-2}. To assess the galvanostatic charging-discharging cycling stability, two identical Zn/ZISG-CC were assembled into Zn|Zn symmetric cells. The capacity of Zn pre-deposition on ZISG-CC was 10 mAh·cm^{-2} (for the low cycling capacity of 0.5 mAh·cm^{-2} and 2.5 mAh·cm^{-2} in symmetric cells and for the charge-discharge cycling in full cells) and 20 mAh·cm^{-2} (for the high cycling capacity of 5 mAh·cm^{-2} and 10 mAh·cm^{-2}). The electrochemical tests of full cells (Zn|MnO_2-graphite, Zn/ZISG-CC|MnO_2-graphite) were carried out on 2032 coin-type cell. The MnO_2-graphite cathode were prepared via a blade-casting method using a mixed slurry that consisted of MnO_2-graphite, conductive carbon and PVDF with the mass ratio of 7:2:1 in NMP. The average mass of active material on each cathode electrode was 1.5~2.0 mg·cm^{-2}.

Electrochemical impedance spectroscopy (EIS, frequency range from100 kHz to 0.05 Hz) and cyclic voltammetry (CV, scan rate of 0.2 mV/s) were performed on CHI 660E workstation.

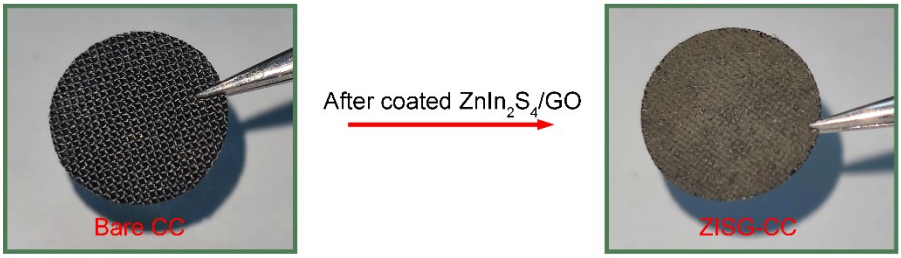

Figure S1. The optical photos of the bare CC and the ZISG-CC.

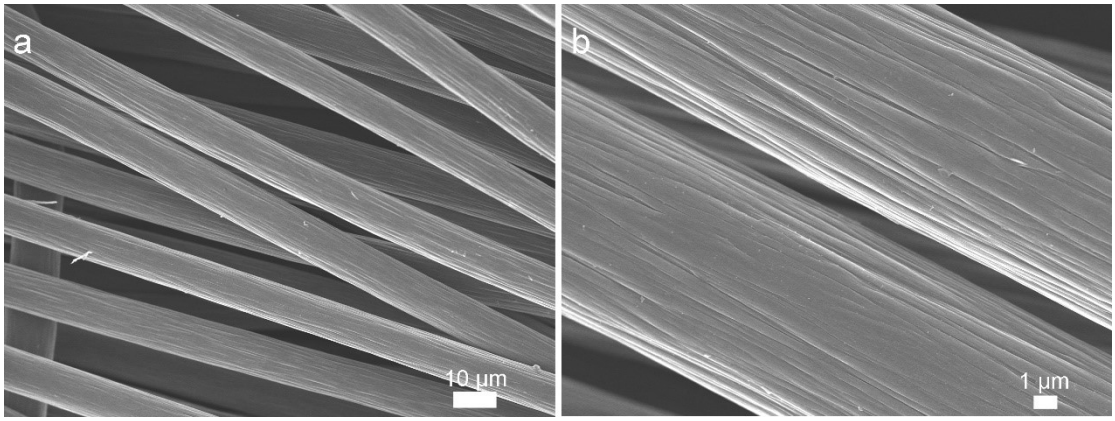

Figure S2. SEM images of CC observed at (a) low and (b) high magnification.

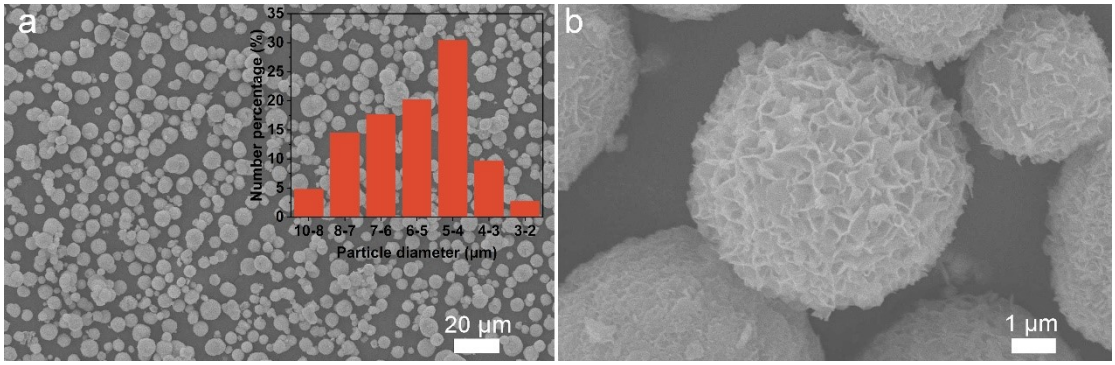

Figure S3. SEM images of the pristine $ZnIn_2S_4$ nanoflowers with the diameter distribution.

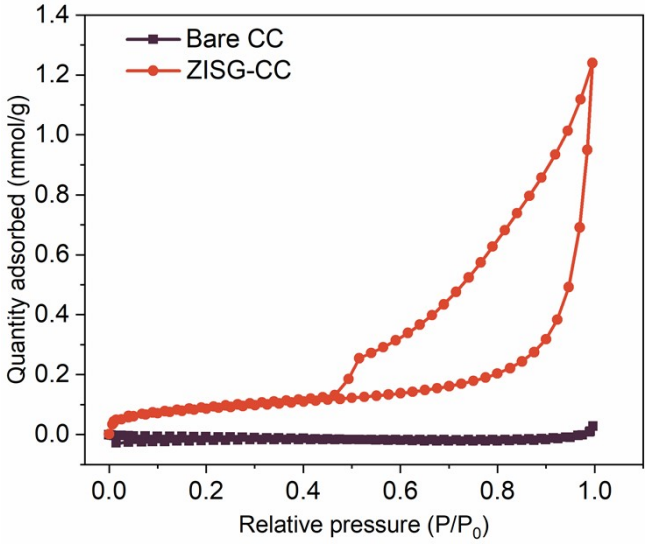

Figure S4. The N_2 absorption-desorption isotherms of the bare CC and ZISG-CC.

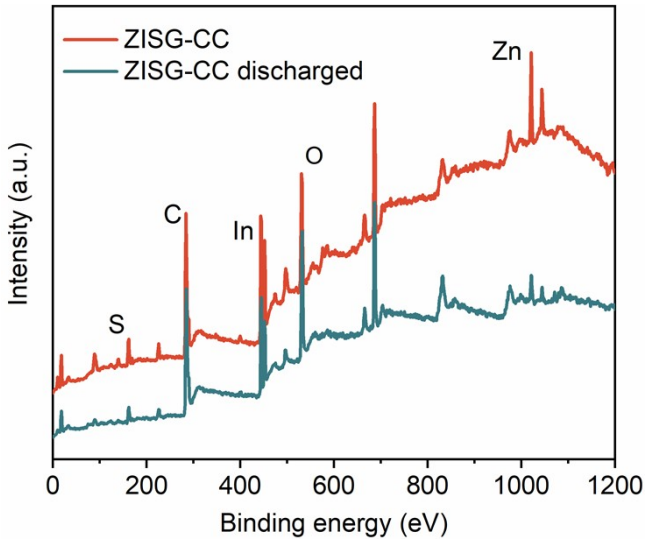

Figure S5. Survey scan XPS spectra of ZISG-CC before and after discharged.

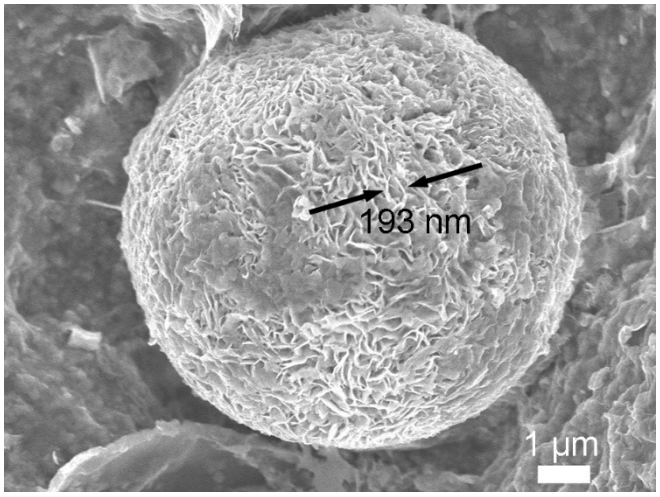

Figure S6. The SEM morphology of ZISG-CC after the voltage decreased to 0V.

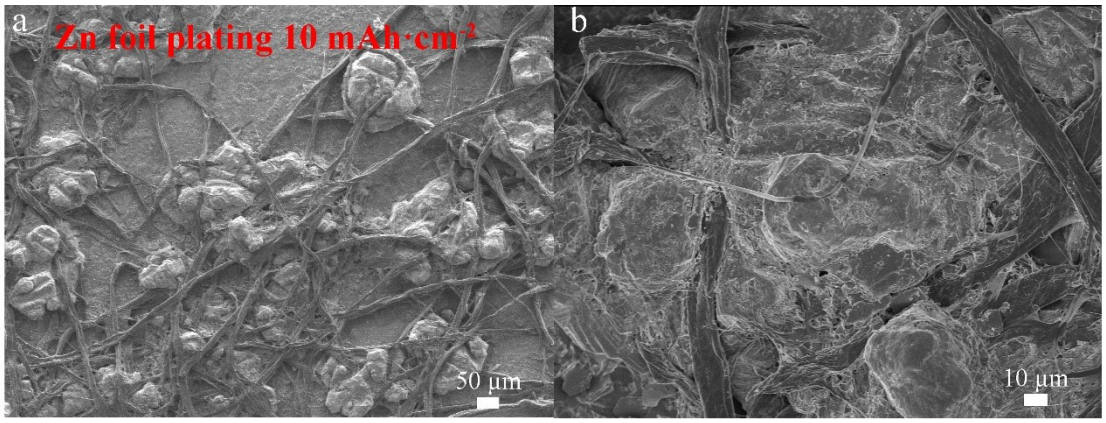

Figure S7. SEM images of Zn deposition on Zn foil and (c, d) bare CC after plating 10 mAh·cm^{-2} of Zn.

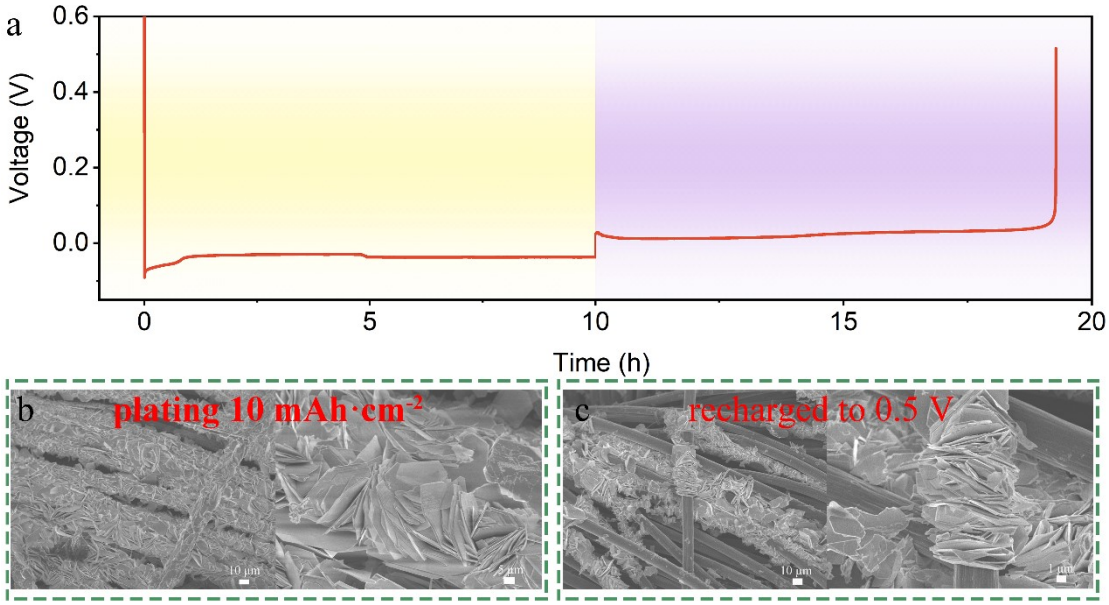

Figure S8. (a) The Voltage-time curve of Zn plating/stripping on bare CC. SEM images of bare CC (b) after plating 10 mAh·cm-2 and (c) after recharged to 0.5 V.

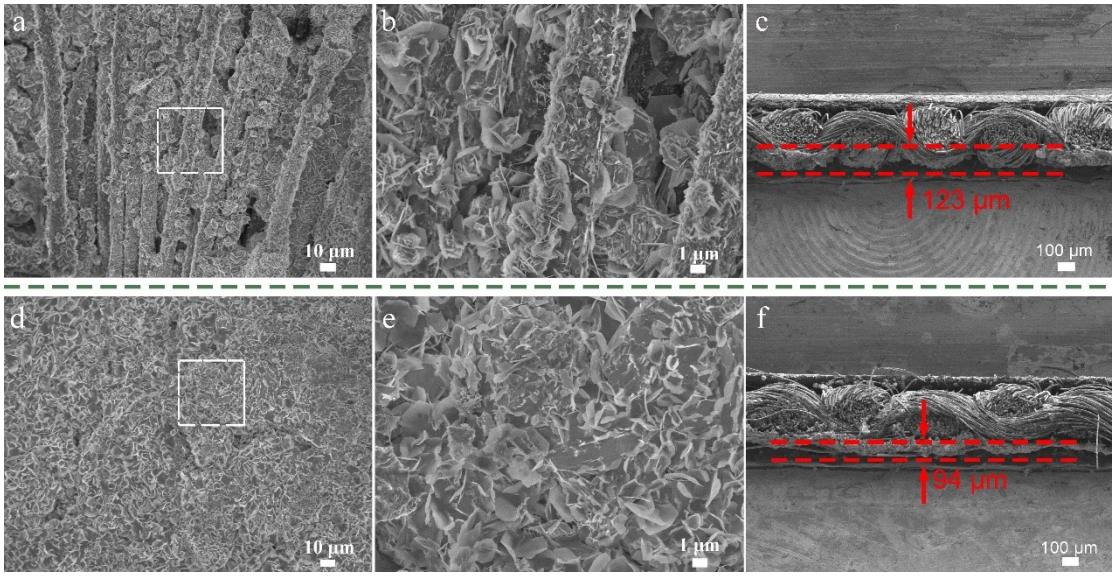

Figure S9. The top view and cross-sectional view SEM images of (a-c) bare CC and (d-f) ZISG-CC after plating 20 mAh·cm^{-2} of Zn.

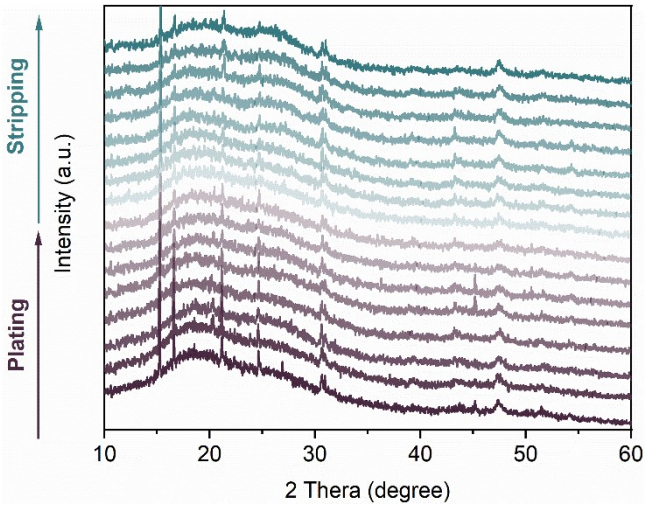

Figure S10. The corresponding in-situ XRD patterns of ZISG-CC during Zn plating/stripping process at 5 $mA \cdot cm^{-2}$ with the capacity of 5 $mAh \cdot cm^{-2}$.

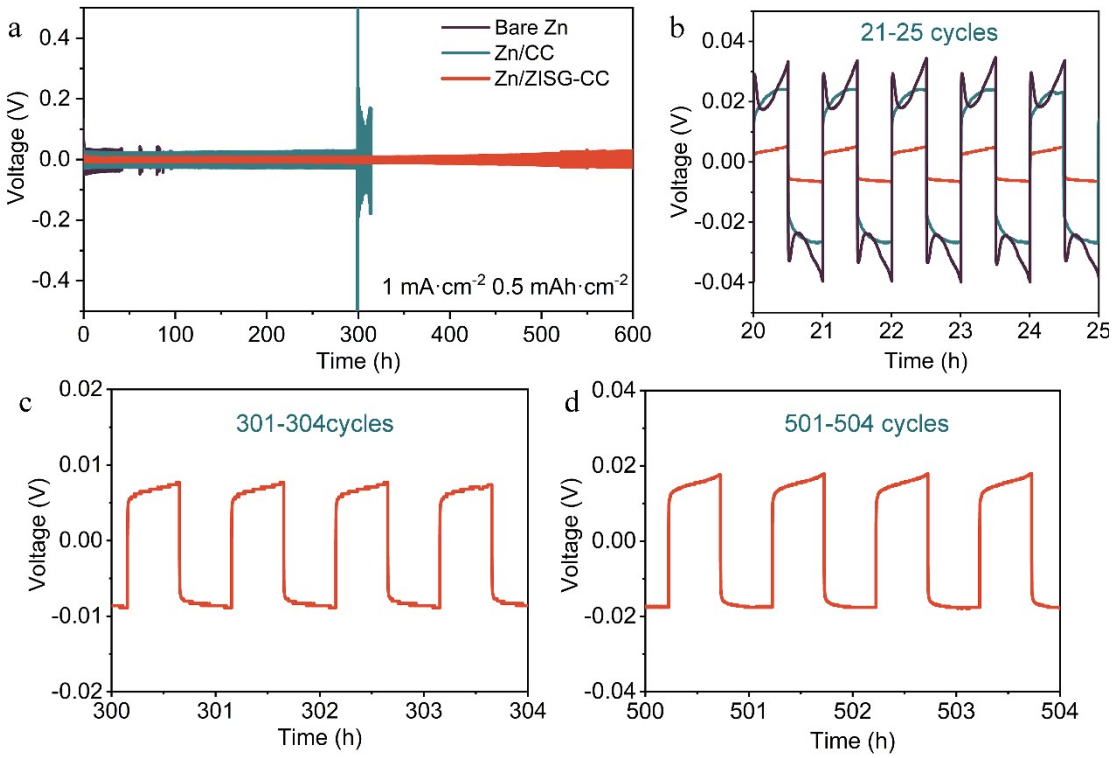

Figure S11. (a) The galvanostatic charge-discharge cycling of bare Zn, Zn/CC and Zn/ZISG-CC at the cycling condition of 1 mA·cm^{-2}/0.5 mAh·cm^{-2} with (b-d) the corresponding voltage hysteresis.

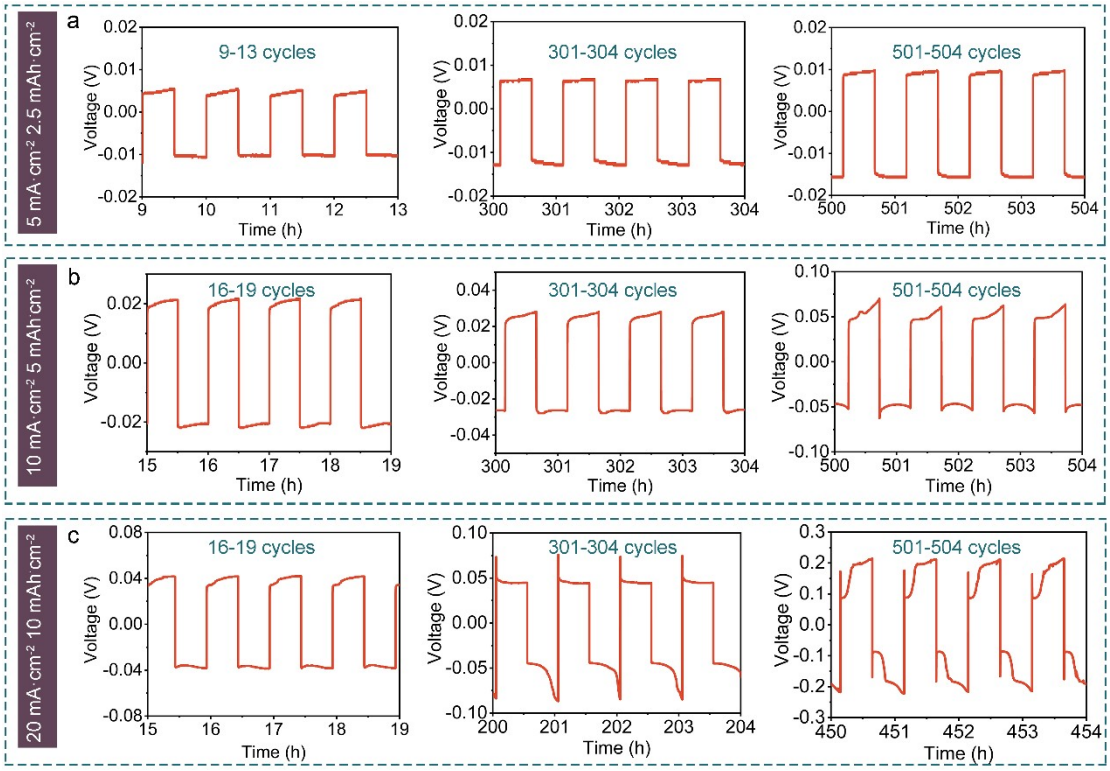

Figure S12. Voltage profiles of Zn/ZISG-CC symmetric cell at (a) 5 mA·cm^{-2}/2.5 mAh·cm^{-2}, (b) 10 mA·cm^{-2}/5 mAh·cm^{-2} and (c) 20 mA·cm^{-2}/10 mAh·cm^{-2}.

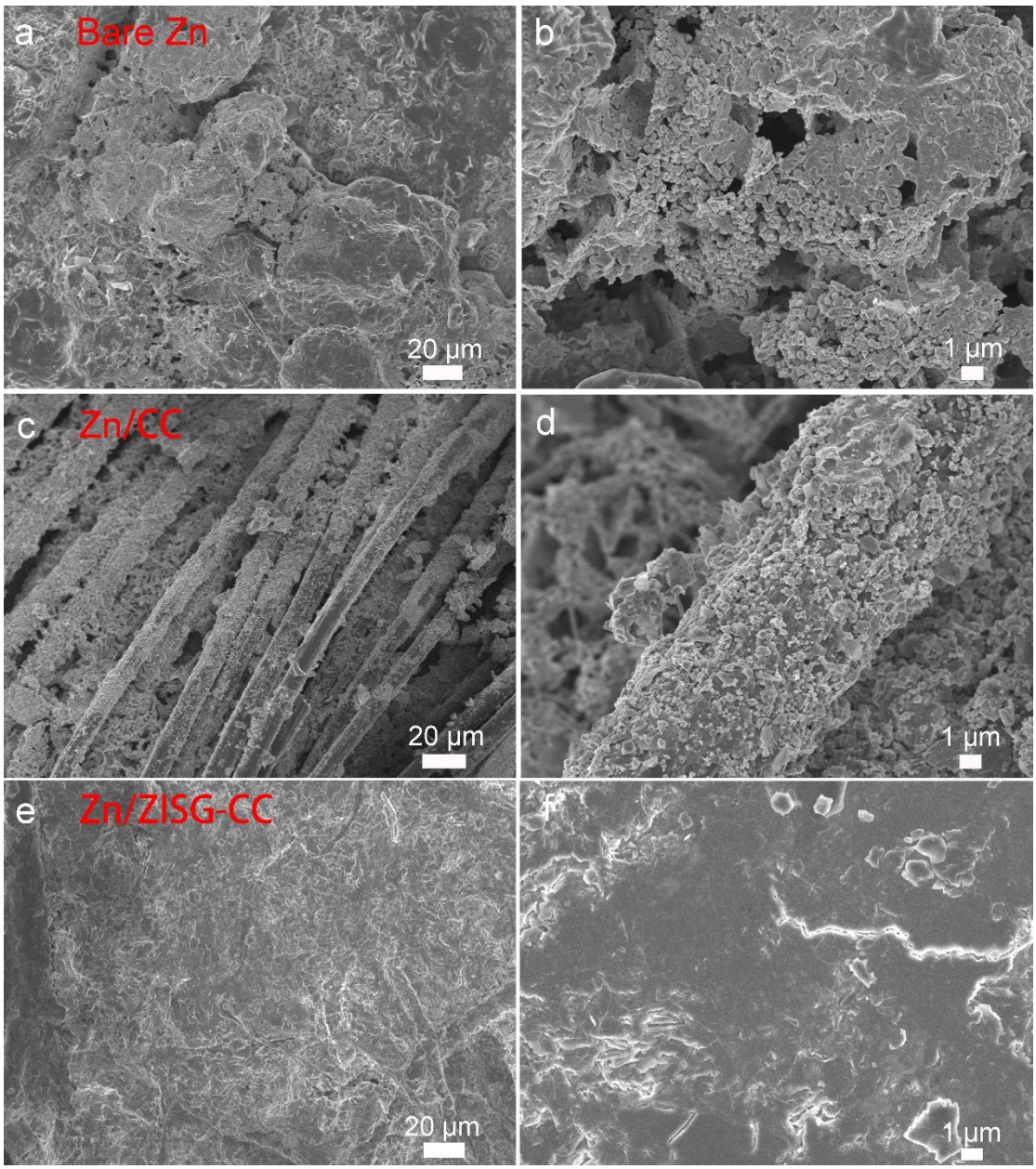

Figure S13. SEM images of (a, b) the bare Zn, (c, d) Zn/CC and (e, f) Zn/ZISG-CC anode after 100 charge-discharge cycles at 5 $mA \cdot cm^{-2}$/2.5 $mAh \cdot cm^{-2}$.

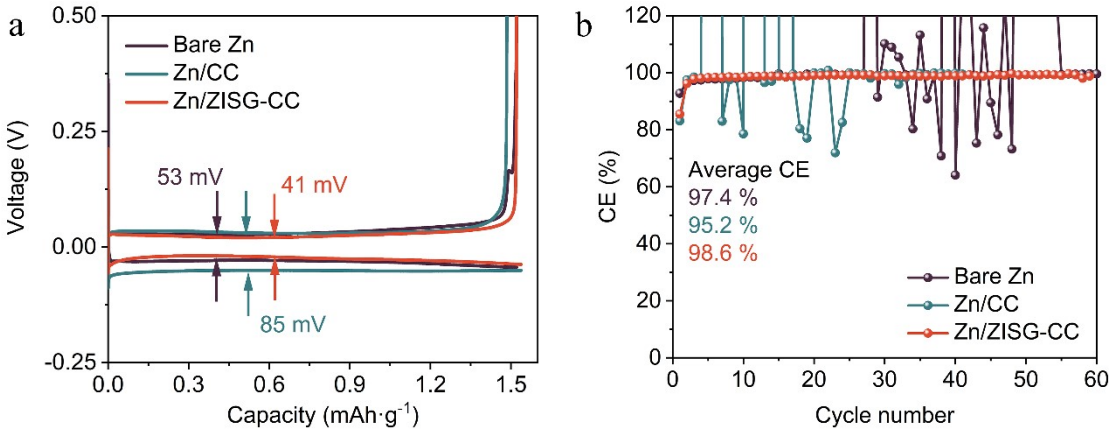

Figure S14. (a) The nucleation overpotentials of Zn on the bare Zn, Zn/CC and Zn/ZOSG-CC anodes with (b) the corresponding average CE value.

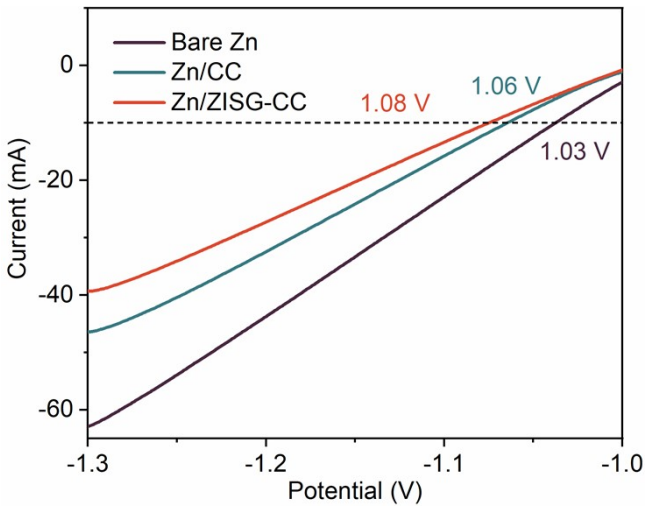

Figure S15. The LSV results of bare Zn, Zn/CC and Zn/ZISG-CC anodes.

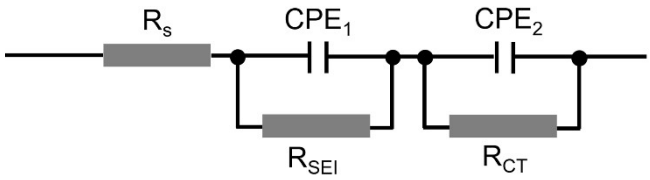

Figure S16. The equivalent circuit of Nyquist plots.

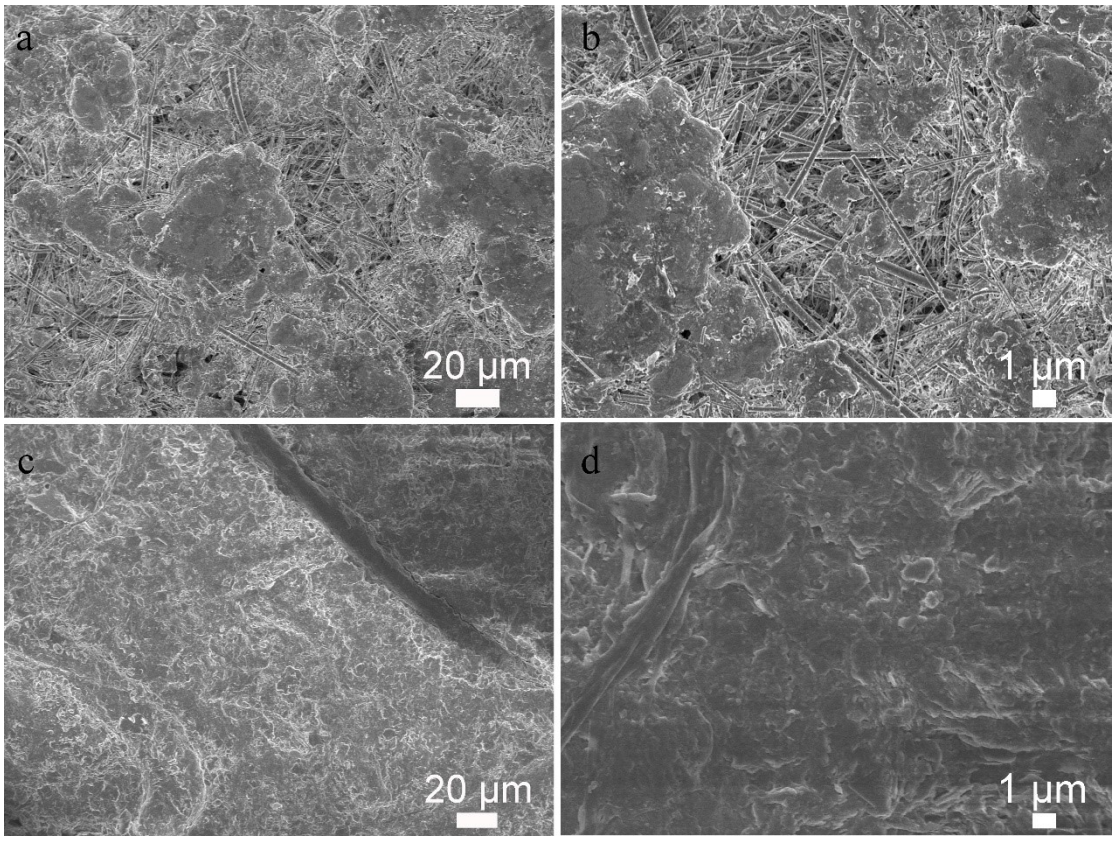

Figure S17. SEM images of (a, b) the bare Zn and (c, d) Zn/ZISG-CC anodes after cycling in the full cells.

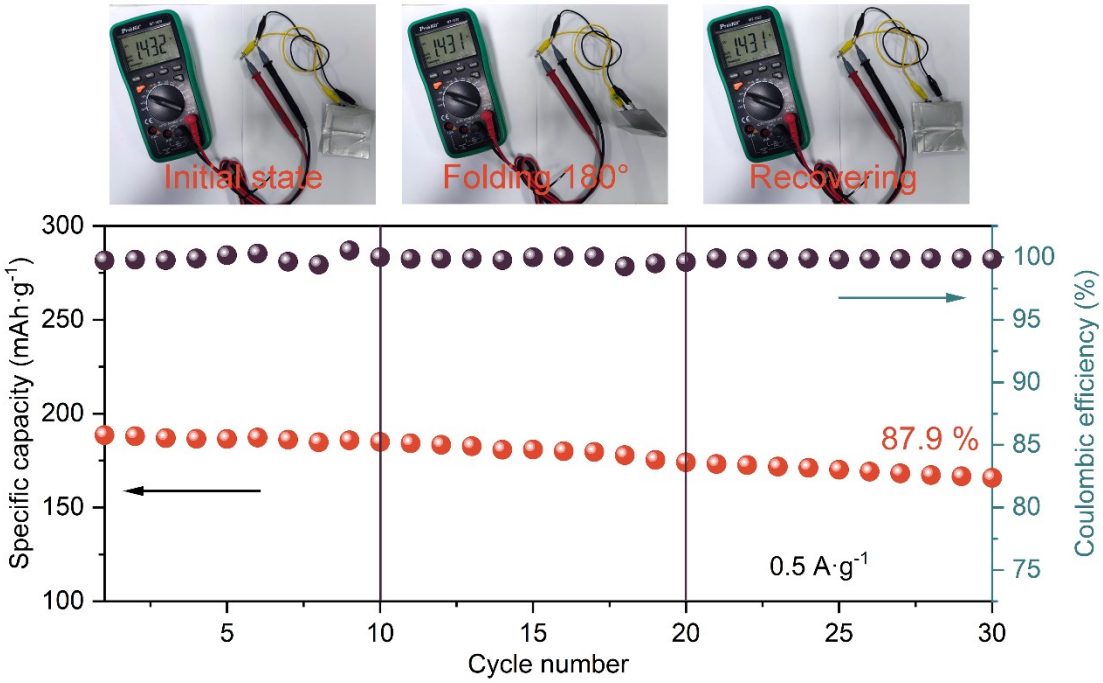

Figure S18. The discharge capacity and the coulombic efficiency of the Zn/ZISG-CC|MnO_2-graphite pouch cell under different states.

Table S1 The stimulated electrolyte resistance (R_S), SEI resistance (R_{SEI}) and charge-transfer resistance (R_{CT}) for bare Zn, Zn/CC and Zn/ZISG-CC anodes.

Anode	$R_s(\Omega)$	$R_{SEI}(\Omega)$	$R_{CT}(\Omega)$
Bare Zn	4.0	550.9	371.9
Zn/CC	3.4	18.1	251.2
Zn/ZISG-CC	3.1	9.7	22.5

References

1. J. Cao, D. Zhang, X. Zhang, S. Wang, J. Han, Y. Zhao, Y. Huang and J. Qin, *Applied Surface Science*, 2020, **534**, 147630.